COMPUTATIONAL SIMULATION, MULTI-SPECTROSCOPIC AND DEGRADATION ANALYSIS OF THE INTERACTION BETWEEN *Trametes versicolor* LACCASE AND BISPHENOL *E*

Xiaolian Lin [1,2], Hongyan Liu [1,2*], Minhua Xu [1,2], Mengjie Shi [1,2], Zhongsheng Yi [2], Litang Qin [3], Huiying Chen [2]

[1] Guangxi Key Laboratory of Electrochemical and Magneto-Chemical Functional Materials, Guilin, China; e-mail: lhyglite@126.com
[2] College of Chemistry and Bioengineering, Guilin University of Technology, Guilin, China
[3] The Guangxi Key Laboratory of Theory and Technology for Environmental Pollution Control, Guilin, China

Trametes versicolor laccase, one of the main enzymes used for the biodegradation of environmental pollutants, has received much attention in the degradation of phenolic pollutants. In this study, the binding energy between the Trametes versicolor laccase and bisphenol E (BPE) is first calculated by means of computational simulation. Moreover, the interaction between Trametes versicolor laccase and bisphenol E is studied with multi-spectroscopy. The results show that bisphenol E can be effectively degraded by crude Trametes versicolor laccase under optimal incubation conditions. The kinetic study is used to characterize the kinetic features of the laccase-catalytic degradation of BPE. The calculation results suggest that the reaction can proceed spontaneously. Spectral analyses show that the secondary structure of laccase is changed after the interaction between laccase and bisphenol E. The degradation efficiency of BPE is up to 93.64% after reacting for 6 h, and the maximum catalytic reaction rate is 0.1764 mg/(L·min). The reactions follow a first-order kinetic equation when the initial concentration of the substrate is lower than 5 mol/L.

Keywords: *bisphenol E, computational simulation, degradation, spectral analysis, Trametes versicolor laccase.*

КОМПЬЮТЕРНОЕ МОДЕЛИРОВАНИЕ, МУЛЬТИСПЕКТРОСКОПИЧЕСКИЙ И ДЕГРАДАЦИОННЫЙ АНАЛИЗ ВЗАИМОДЕЙСТВИЯ ЛАККАЗЫ *Trametes versicolor* С БИСФЕНОЛОМ *E*

X. Lin [1,2], H. Liu [1,2*], M. Xu [1,2], M. Shi [1,2], Z. Yi [2], L. Qin [3], H. Chen [2]

УДК 543.42:577.15

[1] Главная лаборатория электрохимических и магнитохимических функциональных материалов Гуанси, Гуйлинь, Китай; e-mail: lhyglite@126.com
[2] Колледж химии и биоинженерии Гуйлиньского технологического университета, Гуйлинь, Китай
[3] Главная лаборатория теории и технологии контроля загрязнения окружающей среды Гуанси, Гуйлинь, Китай

(Поступила 5 апреля 2021, в окончательной редакции — 23 мая 2022)

Взаимодействие между лакказой Trametes versicolor, одного из основных ферментов, используемых для биоразложения загрязнителей окружающей среды, и бисфенолом E (BPE) изучено с помощью компьютерного моделирования и мультиспектрального анализа. Показано, что BPE может эффективно разлагаться сырой лакказой Trametes versicolor при оптимальных условиях инкубации. Кинетическое исследование использовано для характеристики кинетических особенностей лакказно-каталитической деградации BPE. Результаты расчетов свидетельствуют о том, что реакция может протекать самопроизвольно. Спектральный анализ показывает, что вторичная структура лакказы изменяется после взаимодействия лакказы с BPE. Эффективность разложения BPE составляет ≤93.64% после реакции в течение 6 ч, максимальная скорость каталитической реакции

— 0.1764 мг/(л·мин). Реакции описываются кинетическим уравнением первого порядка, когда начальная концентрация субстрата <5 моль/л.

Ключевые слова: *бисфенол Е, численное моделирование, деградация, спектральный анализ, лакказа Trametes versicolor.*

Introduction. Environmental hormones, also known as endocrine-disrupting substances or environmental estrogens, are released into the environment because of human production and life [1]. Of particular concern are endocrine-disrupting chemicals (EDCs), exogenous compounds that can affect hormonal pathways involved in the development and function of both male and female reproductive systems [2]. They can replace hormones in humans or animals, affecting normal hormone levels, causing endocrine imbalances, and seriously threatening the reproduction and survival of humans and other species [3]. Bisphenol E (bis(4-hydroxy phenyl)ethane), BPE), as an alternative to bisphenol A, is one of the typical environmental endocrine disrupting compounds (EDCs) [4–6]. A small intake of BPE can damage the human endocrine system, resulting in infertility and birth defects. The biological toxicity and the endocrine-disrupting activity of BPE are equivalent to that of bisphenol A [4]. Therefore, finding effective ways of disposing of BPE is critical to humans.

Laccase (EC.1.10.3.2), which can be used to degrade endocrine disruptors, is oxygen oxidoreductase containing copper ions mainly distributed in plants, microorganisms, fungi, and bacteria [7–10]. Its unique copper ion can transmit electrons in the structure, which endows the laccase with unique redox ability. Laccase can interact with various substrates such as lignin, amine compounds, aromatic compounds, and the final degradation product of laccase is water [11–13]. Fungal laccase has certain advantages over bacterial laccase on account of its high efficiency in pollutant degradation and low nutrition requirements [14–16]. *Trametes versicolor* laccase (*T. versicolor* laccase), as one of the fungal laccases for green biocatalysts, has broad application prospects in wastewater treatment and soil remediation [17–21].

The interaction between *T. versicolor* laccase and BPE is characterized by computational simulations, multispectral analysis and degradation experiments. This work focuses on studying the binding mode between *T. versicolor* laccase and BPE at a molecular level, the interaction type is determined by multispectroscopic methods, and the binding ability of *T. versicolor* laccase to BPE is evaluated by degradation experiments. We hope that the mechanism proposed in this study can further provide a theoretical basis and referential information for the study of catalytic exogenous substances of *T. versicolor* laccase, which is important for exploring the degradation ability of *T. versicolor* laccase and reducing the formation of BPE.

Materials and methods. *T. versicolor* laccase (0.5 U/mg, CAS: 80498-15-3) was purchased from Shanghai Ye Yuan Biotechnology Co. Ltd (Shanghai, China). The BPE, sodium acetate (anhydrous) and acetic acid were obtained from Xilong Scientific Co., Ltd. (Shantou, China). The buffer solution (pH 5.5) was prepared by mixing appropriate acetic acid (1 M) with sodium acetate (1 M). The BPE were dissolved in a small amount of methanol to 1.0×10^{-6} mol/L. The laccase was diluted with acetate–acetate buffer solution (pH 5.5) to 1.0×10^{-5} mol/L. All other reagents were analytically pure, and the water was double-distilled water. Molecular docking of BPE with laccase was performed by Autodock 4.2 software using the Lamarckian genetic algorithm. The small molecular structure of the ligand (BPE) was first drawn and optimized using ChemBioDraw Ultra software [22]. The three-dimensional structure of the laccase (PDB id: 1GYC) was downloaded from the Protein Data Bank (http://www.rcsb.org./pdb) [23]. According to the molecular docking, the chemical bonds in the molecule were precisely processed and saved as a file in pdbqt format containing key information such as atomic coordinates, AutoDockTools atom types, charges, and distortable bonds [24, 25]. The size of the docking grid was fixed at 100×100×100 Å, and the grid energy was calculated by Autogrid. The binding of laccase to BPE was evaluated by the semi-empirical free energy calculation method ENREF_41 [26]. The binding energy is closely related to the binding affinity, and low binding energy shows strong affinity [27]. Ligplus^{+} software was used to study the interaction between laccase and BPE [28].

The molecular dynamics simulation (MD) of the BPE and laccase system in a timescale of 20 ns was carried out using GROMACS 4.5.5 software. Laccase proteins were downloaded from the RCSB website for optimization by SYB-X after the removal of self-ligands. The ligand was optimized using ChemBioDraw Ultra software and then converted to ligand topology files via the online platform (The PRODRG Server). The topology files in gro format were used for molecular dynamics simulations. In the MD, the force field was set to GRO-MOS96 43 A1. The structure of the optimized protein was used as a reference. The SPC water model and cubic water box (new box) were used with a minimum distance between the protein and the water box wall of 1 nm. If the total system charge was negative, Na+ ions were added. Otherwise, Cl^{-} ions

were added to balance the charge. The steepest descent method was used for energy minimization of the initial structure. The canonical ensemble (NVT) and NPT ensemble were used to equilibrate the system. Finally, the results were analyzed using Origin software.

The fluorescence spectra were collected using a Cary Eclipse fluorophotometer (Varian, CA, USA). In the fluorescence experiment, the excitation wavelength was 280 nm. The emission spectra were recorded between 280 and 450 nm. The fluorescence experiments were conducted at three different temperatures (298, 303, and 310 K). The excitation and the emission slit widths were 5 nm. Reactions were carried out under the aforementioned conditions. In the cuvette, 2 mL of laccase stock solution (1×10^{-5} mol/L) and BPE stock solution (1×10^{-7} mol/L) with different volumes (10, 20, 40, 60, 80, and 100 μL) were added.

The UV-visible spectrophotometer (TU-1950; Beijing Purkinje General Instrument Co., Beijing, China) was used for the acquisition of UV-visible spectra. The enzyme stock solution (2 mL, 1×10^{-5} mol/L) was transferred into a colorimetric tube followed by the addition of BPE solution with different volumes. The UV spectrophotometer was applied to determine the UV absorption spectrum of the samples within the wavelength range 190–400 nm.

The Fourier transform infrared spectrometer iS10 was from Thermo Fisher Company. Samples were prepared via potassium bromide (KBr) tableting. The solutions of laccase and BPE–laccase were subjected to infrared spectroscopy by using the liquid coating method.

Based on previous work, a degradation experiment was carried out under optimal degradation conditions (27.5°C and pH 5.5) [22]. The degradation efficiencies at 0.5, 1, 3, 6, 12, and 24 h were tested. Then, the effect of temperature 20, 27.5, 35, 42.5, and 50°C on the degradation efficiency of BPE by crude laccase solution was investigated. Results were obtained from three parallel measurements. One milliliter of crude laccase was used in each experiment.

Degradation experiments were implemented under optimized conditions for laccase culture. The effect of pH of the reaction system on the BEP degradation by laccase was investigated within the range 4.0 to 7.5. The influence of substrate concentrations ranging from 5 to 50 mol/L on the degradation efficiency of BPE was studied. Each test contained three parallel experiments and consumed 1 mL of crude laccase solution.

The reaction system consisted of 1 mL of laccase solution and different volumes of BPE stock solution. The final substrate concentrations were composed of 1, 5, 10, 15, and 20 mg/L. Its pH remained at 5.5. Then, the resulting system was cultured in an oscillating incubator at 27.5°C. The concentration of substrate in the system was determined after degradation of 1, 2, 3, 4, 5, and 6 h. Three parallel experiments were performed for each test.

Results and discussion. *Computational simulations.* Molecular docking is often used to reveal the binding of small ligand molecules with receptor macromolecules, and to screen the best structure and conformation [29, 30]. Therefore, it is considered a valuable simulation method to predict the preferred conformation of BPE binding to the laccase. Molecular docking results show that the binding energy between BPE and laccase in the optimal conformation was −7.56 kcal/mol. The negative value suggests that the reaction can proceed spontaneously. The results of molecular docking of laccase and BPE are marked in Fig. 1. The optimal binding site of laccase for BPE is shown in Fig. 1a. In Figure 1b, BPE is embedded in the hydrophobic cavity of laccase and mainly surrounded by key amino acids such as Val 82, Pro 79, Phe 450, His 111,

Fig. 1. Molecular docking results of the BPE–laccase complex: (a) the second structure of laccase in the docking simulation; (b) amino acid residues and the type of interaction between BPE and laccase; (c) two-dimensional representation of the interaction maps between BPE with participation of several active amino acid residues of laccase.

Ser 113, Leu 459, Pro 346, Thr 345, Phe 344, Glu 460, and Ala 80, resulting in different degrees of hydrophobicity of the BPE towards laccase. Through Ligplus^{+} analysis of eyelash images, it can be concluded that BPE forms hydrogen bonds with Phe 344 and Ala 80 residues in laccase, which makes laccase more stable. Details of the hydrogen bonding are shown in Fig. 1c. Small molecules and laccase form a fully encapsulated hydrophobic interface, which strengthens the interaction between them. It can be seen that the interaction between laccase and BPE is enabled by hydrogen bonds and hydrophobic force [31].

Molecular dynamics simulation can study the stability and kinetics of small complex molecules in an aqueous solution. To explore the conformational stability and effective conformational sampling of laccase during MD simulations, root-mean-square deviation (RMSD), the deviation statistics of the resultant conformation and the target conformation, is calculated based on the starting structure. Figure 2a illustrates the RMSD of laccase and the laccase-BPE complex for 20 ns. The fluctuation of the compound is ambiguous. In the first 10 ns, the RMSD of the complexes is higher than those of the free protein. The results show that BPE interacts with laccase, and that the hydrogen bonds and hydrophobic forces contract the entire secondary structure. After 10 ns, the binding between laccase and BPE reaches a stable state and the radius of gyration (R_g) value of the complex is gradually lower than that of the free laccase. This result suggests that the binding of BPE to laccase might alter the protein structure of laccase, and also demonstrates that the complex is stable and more tightly bonded after the binding of BPE with laccase, which promotes the homeostasis of the laccase–BPE complex system and the contraction of the helical structure of amino acids.

The R_g is predicted to analyze the compactness of the target protein and the entire structure of a protein. A smaller R_g value shows a tighter structure in a specific region of the protein and vice versa. As seen in Fig. 2b, the R_g value of the overall complex was smaller than that of the free laccase. The interaction of BPE with laccase results in the contraction of the entire secondary structure by the mutual attraction between the residues of laccase. Hydrogen bonding forces and hydrophobic forces generated by BPE and laccase make the complex more compact. Then, the alteration of the microenvironment leads to a change in the protein's conformation. These results indicate that BPE changes the spatial structure of the protein, thus causing the system to expand, then contract, and finally stabilize, which is corroborated by the RMSD plot.

The root-mean-square fluctuation (RMSF) provides information about the fluctuations per residue of protein–ligand complexes. The larger the RMSF, the greater the fluctuations, indicating more pronounced changes in amino acid residue positions during MD simulations, and greater elasticity and increased fluctuation in magnitude and flexibility. As shown in Fig. 2c (20 ns), the RMSF value of laccase is larger than that of the laccase–BPE complex, indicating that the enzyme produces a tight complex with the ligand.

The RMSF plot showed fewer fluctuations of the atoms in the laccase–BPE complex, suggesting that the amino acid residues of the protein remained stable throughout the simulation. I and II of the RMSF show that the complex has two different regions with high fluctuations (residues 296–375, 395–473). The RMSFs of these two regions of the complex are higher than those of the free laccase, suggesting that the formation of the laccase–BPE complex might lead to a change in the structure of the laccase, which has more flexibility. It is speculated that the interaction between BPE and laccase may have a greater influence on the residues in this range, affecting the surrounding environment and then the secondary structure of the protein.

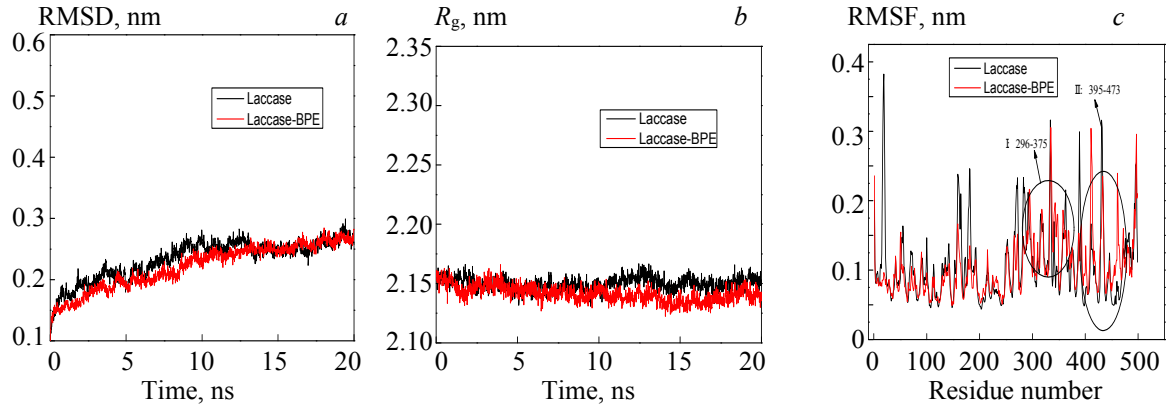

Fig. 2. (a) Root-mean-square deviation (RMSD), (b) radius of gyration (R_g), (c) root-mean-square fluctuation (RMSF) of laccase and the laccase–BPE complex from 20 ns of MD simulations.

Spectral analysis. Through the quenching experiment, the fluorescence spectra before and after the binding can be compared to determine the overall structure change of the enzyme molecule [32]. In the spectroscopy experiments, alternation in fluorescence signal could determine whether or not the ligand is bound to the receptor. Proteins can fluoresce because of the presence of three aromatic amino acids Trp, Tyr, and Phe [33]. The fluorescence quenching process of binding interaction is always divided into static and dynamic (collisional) quenching and nonradiative energy transfer. The quenching type, binding constant and site can be calculated by the Stem–Volmer and double logarithmic curve equations [34, 35].

$$F_0 / F = 1 + K_{SV}[Q] = 1 + K_q \tau_0 [Q], \quad (1)$$

$$\log(F_0 - F) / F = \log K_a + n \log[Q], \quad (2)$$

where F_0 and F are the fluorescence intensities in the absence and the presence of BPE, respectively; K_{SV} is the Stern–Volmer dynamic or collisional quenching constant, which represents the efficiency of quenching; K_q is the quenching rate constant or bimolecular quenching constant; τ_0 is the average lifetime of the fluorophore without quencher and its value is considered to be 10^{-8} s; K_a is the apparent binding constant, and n is the number of binding sites.

Figure 3a shows that with the increase in BPE concentration, the fluorescence intensity at 310 K decreases. Assuming that the quenching process is dynamic quenching, K_q decreases with the increase in temperature in Fig. 3b, and the K_q value of laccase to BPE is much larger than the maximum dynamic quenching constant 2.0×10^{10} L · mol^{-1} · s^{-1} of various quenchers for biological macromolecules. The result is contradictory to the hypothesis and conforms to the static quenching mechanism. This elucidates that BPE enters the hydrophobic cavity of laccase, and forms a nonfluorescent complex with laccase, which causes the protein conformational changes, finally leading to fluorescence quenching of laccase. The binding constants (K_a) and binding sites (n) of the interactions are calculated according to the double logarithm curve of the laccase–BPE system at different temperatures in Fig. 3c. It can be seen from Table 1 that the number of binding sites n is about 1, indicating that laccase binds with BPE in a 1:1 equivalent. The binding constant of laccase decreases along with the increasing temperature, which further proves that the fluorescence quenching of laccase and BPE is static quenching.

Proteins exhibit mainly characteristic ultraviolet (UV) absorption peaks in the presence of tyrosine and tryptophan [36], which facilitates the characterization and analysis of the structural integrity of proteins without damaging the sample. UV-Vis absorption spectroscopy is used to evaluate the parameters, such as binding constant and free energy of interaction, and reflects the change in the macromolecular structure of protein based on the change of absorption peak [37]. The absorbance of protein from Tyr and Trp residues depends on the chromophore microenvironment [38]. The decrease in absorbance is accompanied by a blue shift in its maximum absorption peak [39]. The UV absorption spectra of BPE and laccase are shown in Fig. 4. Increasing the BPE concentration continuously increases the blue shift of the absorption peak. With the increase in polarity in the residues around the protein, the peptide chain extends more, resulting in a variation in the secondary structure of laccase. The decreasing UV absorption peak suggests that BPE and laccase might have a hypochromic effect, and the DNA double helix structure of the protein is transformed during the interaction. The results show that the BPE affects the secondary structure of the laccase and forms a complex between them.

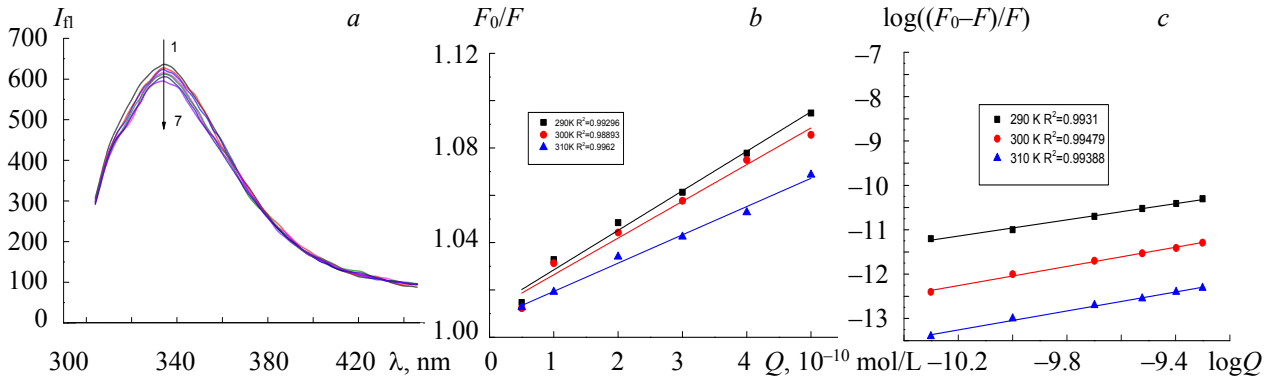

Fig. 3. (a) Fluorescence quenching diagram of BPE to laccase (pH 5.5, T = 310 K, λ_{em} = 280 nm); (b) Stern–Volmer curve of the laccase–BPE system at different temperatures; (c) double logarithm curve of the laccase–BPE system at different temperatures.

TABLE 1. The Fluorescence Quenching Constant, Binding Constant, and Site of Laccase–BPE Interaction at Different Temperatures

T, K	K_{SV}, 10^4 L/mol	K_q, 10^{12} L/(mol·s)	K_a, 10^5 L/mol	n
290	1.67077	1.67	2.34784	0.91431
300	1.55162	1.55	1.81668	1.0956
310	1.19551	1.96	1.23419	1.08078

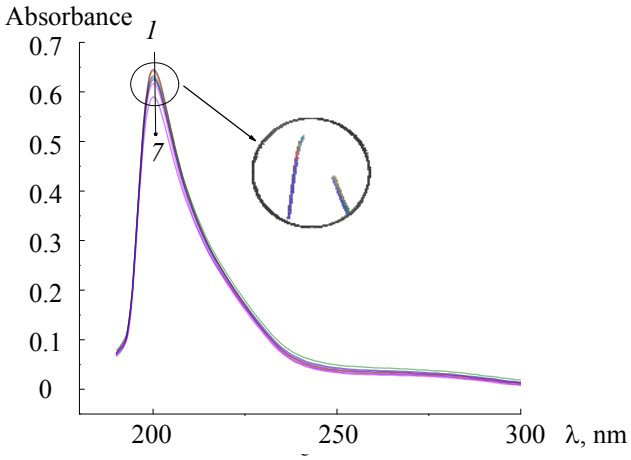

Fig. 4. UV absorption spectra of the laccase system with different concentrations (1–7) of BPE.

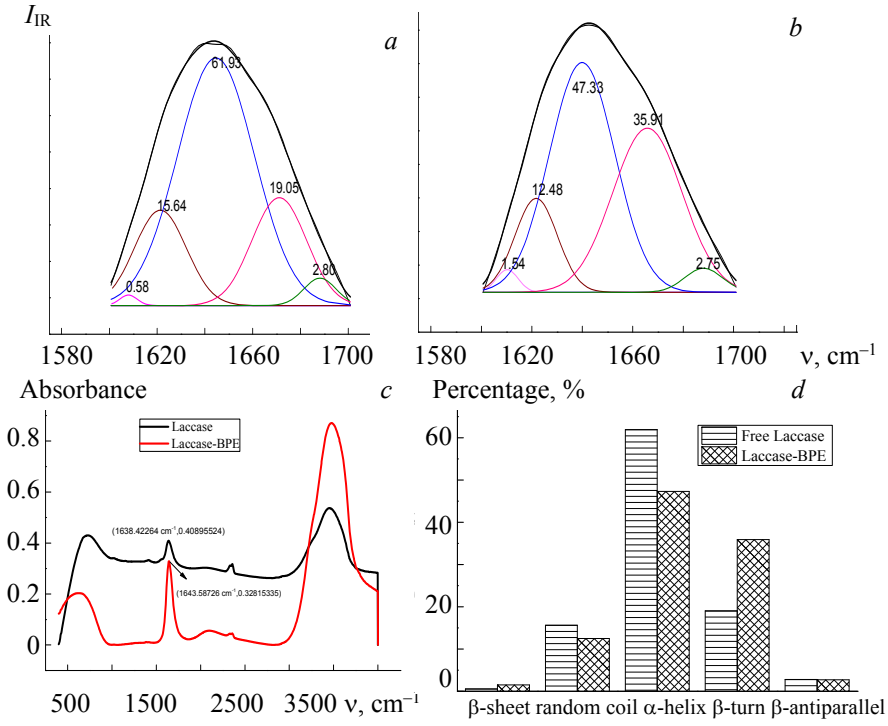

Fig. 5. The infrared spectra of (a) free laccase and (b) laccase–BPE from 1600 to 1700 cm^{-1}; (c) the free laccase and the laccase–BPE complex from 500 to 4000 cm^{-1}; (d) percentage of laccase and laccase–BPE secondary structures determined by FT-IR spectroscopy.

Infrared spectroscopy was applied to investigate the secondary structures [40]. Figure 5 shows the IR spectra of the BPE–laccase complexes. The characteristic absorption peaks for the secondary structure are mostly at 1600–1700 cm^{-1} (amid I band). The amid I band is the most frequently used band to infer the secondary structure of peptides as it arises (80%) from the backbone C=O stretching vibration, which is strictly

related to the protein secondary structure [41–43]. The absorption bands at 1615–1637, 1638–1648, 1649–1660, 1661–1680, and 1681–1692 cm^{-1} are commonly assigned to β-sheet, random coil, α-helix, β-turn, and β-antiparallel structure, respectively [43, 44]. Deconvolution and peak fitting were used to process the infrared spectrum from 1600 to 1700 cm^{-1}. The relative percentage of each conformation in the secondary structure of the protein was calculated under area integrals. According to the infrared spectra of BPE and laccase, the protein structure of laccase changes significantly after the interaction with BPE. The percentage of β-sheet and β-turn increases from 0.58 to 1.54% and from 19.05 to 35.91%, respectively. The percentage of random coil, α-helix, and β-strands decreases from 15.64 to 12.48%, from 61.93 to 47.33, and from 2.80 to 2.75%, respectively. Infrared spectroscopy indicates that BPE can induce changes in the secondary structure of laccase proteins and further confirms a strong interaction between laccase and BPE.

Degradation analysis. On the basis that the process could be performed spontaneously, the degradation ability and kinetics of laccase on BPE were investigated by degradation experiments. Figure 6 shows the degradation efficiency of laccase on BPE at different temperatures. The results demonstrate that at the same temperature the degradation efficiency of laccase on BPE soared after 6 h of degradation. The degradation efficiency reached equilibrium at the 12^{th} h. Among them, the highest degradation efficiency was at 27.5°C, when the degradation efficiency was as high as 71.11%, which was slightly lower than that of BPA (80%). Based on the previous work of our laboratory, it was found that the degradation mechanism of BPE by laccase is similar to that of BPA [22].

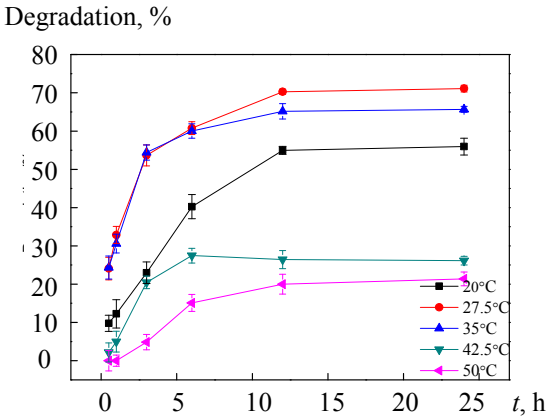

Fig. 6. Degradation efficiencies of BPE as a function of reaction time at different temperatures.

Because of the increase in temperature, the percentage of active molecules in the reaction system escalates, accelerating the movement speed of molecules and ramping up the effective collision time. As a result, the reaction process is sped up. The reasons for the optimal conversion at 27.5°C are as follows: when the temperature is no more than 27.5°C, the reaction rate increases with the increase in temperature at the identical reaction time, leading to the enhancement of degradation efficiency; but when the temperature is higher than 27.5°C, the thermal-induced inactivation of the enzyme accelerates, resulting in a decrease in the amount of active enzymes, and thus a decrease in the degradation efficiency [45, 46]. Therefore, the optimal temperature for BPE degradation is the result of concomitant effects of temperature on the enzyme participated catalytic reaction rate and deactivation rate.

The degradation efficiencies of BPE in the reaction systems with different pH were measured after the BPE was degraded by laccase (10 mol/L) for 1 h at 27.5°C. As shown in Fig. 7, the laccase shows rather low (<20%) degradation efficiency to BPE under low pH. With the increase in pH, the degradation of BPE increases at first and then decreases. The highest degradation efficiency (59.72%) was achieved at pH 5.5. It is presumed that the change of pH of the reaction system affects the biological activity of laccase, then the variation of laccase activity in the system in turn impacts the degradation of substrates. As we all know, enzymes exhibit biological activity within a certain range of pH. Excessive acidity or alkalinity will weaken their enzyme activity and even cause irreversible destruction, which will result in protein denaturation. Different acidity and alkalinity also influence the charged state of substrate and enzyme molecules, which further inhibits or promotes the binding of enzyme to substrate. Therefore, the change of acidity and elasticity in the reaction system significantly influences the degradation of BPE by laccase. The optimal pH is similar

to that of the previous study [47]. The effects of BPE concentration were investigated at pH 5.0 and 27.5°C, and the BPE degradation efficiency was tested after reacting for 1 h. As shown in Fig. 7, the BPE degradation efficiency reaches 84.4% when the initial BPE concentration is 5 mol/L. With the increase in BPE concentration, the BPE degradation efficiency gradually descends to only 28.85% when the BPE concentration is 50 mol/L. Hence, the result indicates that the degradation of BPE by laccase increases from 4.22 to 14.42 mol/L when the substrate concentration increased from 5 to 50 mol/L.

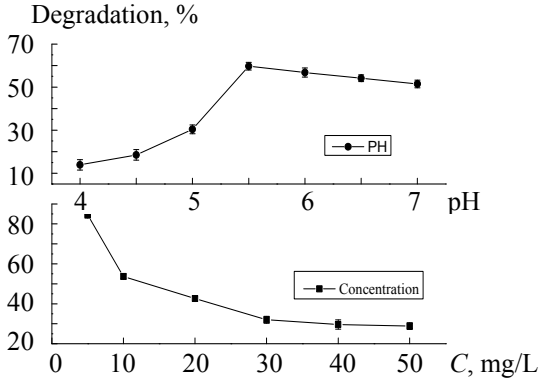

Fig. 7. Effects of pH and substrate concentration on the degradation of BPE.

Kinetic analysis of enzymatic reaction. The equations and parameters for fitting the different concentrations over time are shown in Table 2. When the concentration is 1 mol/L, the reaction occurs too fast to be studied, so the corresponding kinetic equation and parameters are not listed in Table 2. When the BPE concentration ranges from 5 to 20 mol/L, the kinetic equations can be well fitted in first-order and second-order reaction. As seen from Table 2, when the initial BPE concentration was 5 mol/L, the correlation coefficient by fitting in first-order reaction is higher than that in second-order reaction. Thus, the degradation of BPE conforms to the first-order kinetic reaction. The fitting coefficient is higher than 0.95, which suggests that when the substrate concentration is 5 mol/L, the laccase is excessive in the reaction system. According to the kinetic theory of enzyme-catalytic reaction, the reaction rate is proportional to the substrate concentration in the presence of excessive enzyme, and the reaction accords with the first-order kinetics. When the initial BPE concentration is no less than 10 mol/L, higher correlation coefficients are obtained by second-order kinetic fitting. However, the correlation coefficients in first-order kinetic fitting are also higher than 0.95, disclosing that the degradation reactions of BPE belong to mixed-order kinetics. At higher BPE concentration, the amount of laccase is no longer excessive, leading to the decrease in reaction rate.

TABLE 2. Kinetic Equation and Parameters of the BPE

Concentration, mol/L	Kinetic equations	k/[min^{-1} or (mol/L)/min	R^2
5	$\ln Ct = -0.3754t + 0.9197$	0.3754	0.9775
	$1/Ct = 0.5117t - 0.3276$	0.5117	0.9169
10	$\ln Ct = -0.1018t + 1.7453$	0.1018	0.9588
	$1/Ct = 0.2499t + 0.6576$	0.2499	0.9799
15	$\ln Ct = -0.0882t + 2.2635$	0.0882	0.9858
	$1/Ct = 0.1859t + 0.4974$	0.1859	0.9954
20	$\ln Ct = -0.0800t + 2.6467$	0.0800	0.9730
	$1/Ct = 0.1110t + 0.0317$	0.1110	0.9873

N o t e. Ct is the concentration of time t, k is the constant of action.

Conclusions. The interaction of laccase with BPE is studied using computational simulation, multispectroscopic and degradation analyses. The average binding energy of laccase with BPE is −7.56 kcal/mol. On the basis of computational simulation, the main driving forces for the reaction between laccase and BPE were attributed to hydrophobic force and hydrogen bonds. In the spectral experiments, the fluorescence intensity of the laccase–BPE complex shows an upward trend compared with that of the laccase, indicating

that their interaction occurs. The UV and infrared spectra show that BPE interacts with laccase, and the laccase–BPE complex has a different structure from that of free laccase. The effects of BPE on the secondary structure of *T. versicolor* laccase are verified using fluorescence, ultraviolet, and infrared spectroscopy. The optimal conditions for BPE degradation by laccase are obtained at 27.5°C and pH 5.5. After the reaction of 6 h, the optimal degradation efficiency of BPE (5 mol/L) is 93.64%. The maximum catalytic reaction rates of *T. versicolor* laccase to degrade BPE is 0.1764 mg/(L·min). The degradation kinetics study shows that the degradation reaction follows the first-order kinetics equation when the initial concentration of substrate is lower than 5 mol/L. Comprehensively, our results demonstrate that *T. versicolor* laccase has a high affinity with bisphenol E. Further research finds that laccase also has a promising degradation capability to bisphenol E. These results are helpful in deepening our understanding of the interaction mechanism between laccase and BPE. This finding also provides a reference for future studies on conversion and degradation of the other phenolic substances by *T. versicolor* laccase.

Acknowledgements. This work is financially supported by the Research funds of the Guangxi Key Laboratory of Electrochemical and Magneto-chemical Functional Materials (No. EMFM20211113), the National Natural Science Foundation of China (Grant No. 31860251 and No. 21866011) and the Guangxi Key Laboratory of Theory and Technology for Environmental Pollution Control (No. 1701K003).

REFERENCES

1. V. W. Makene, E. J. Pool, *Int. J. Environ. Res. Public. Health*, 16 (**2019**).
2. A. E. Hipwell, L. G. Kahn, P. Factor-Litvak, C. A. Porucznik, E. L. Siegel, R. N. Fichorova, R. F. Hamman, M. Klein-Fedyshin, K. G. Harley, *Human Rep. Update*, **25**, 51–71 (2019).
3. Q. Zhang, C. Ji, X. Yin, L. Yan, M. Lu, M. Zhao, *Environ. Poll.*, **210**, 27–33 (2016).
4. G. H. Wang, F. Wu, *Environ. Chem.*, **25**, 458–461 (2006).
5. M. Y. Chen, M. Ike, M. Fujita, *Environ. Toxic.*, **17**, 80–86 (2002).
6. M. Xiao, J. Q. Xiao, *Water Purif. Technol.*, **28**, 21–24 (2009).
7. C. Y. Bao, Y. Wang, X. L. Xu, D. Li, J. Chen, Z. B. Guan, B. Y. Wang, M. Hong, J. Y. Zhang, T. H. Wang, Q. Zhang, *Bioresour. Technol.*, **342**, 126026 (2021).
8. R. C. Minussi, G. M. Pastore, N. Duran, *Bioresour. Technol.*, **98**, 158–164 (2007).
9. C. Zhang, L. Liu, G.-M. Zeng, D.-L. Huang, C. Lai, C. Huang, Z. Wei, N.-J. Li, P. Xu, M. Cheng, F.-L. Li, X.-X. He, M.-Y. Lai, Y.-B. He, *Biochem. Eng. J.*, **91**, 149–156 (2014).
10. G. Benfield, S. M. Bocks, K. Bromley, B. R. Brown, *Phytochemistry*, **3**, 79–88 (1964).
11. J. A. Majeau, S. K. Brar, R. D. Tyagi, *Bioresour. Technol.*, **101**, 2331–2350 (2010).
12. A. C. Mot, R. Silaghi-Dumitrescu, *Biochemistry (Mos.)*, **77**, 1395–1407 (2012).
13. L. Munk, A. K. Sitarz, D. C. Kalyani, J. D. Mikkelsen, A. S. Meyer, *Biotechnol. Adv.*, **33**, 13–24 (2015).
14. H. Catherine, M. Penninckx, D. Frédéric, *Environ. Technol. Innovat.*, **5**, 250–266 (2016).
15. G. Macellaro, C. Pezzella, P. Cicatiello, G. Sannia, A. Piscitelli, *Biomed. Res. Int.*, 614038 (**2014**).
16. U. N. Dwivedi, P. Singh, V. P. Pandey, A. Kumar, *J. Mol. Catal. B Enzym.*, **68**, 117–128 (2011).
17. M. Asgher, A. Wahab, M. Bilal, H. M. N. Iqbal, *Waste Biomass Valorization*, **9**, 2071–2079 (2017).
18. S. Beck, E. Berry, S. Duke, A. Milliken, H. Patterson, D. L. Prewett, T. C. Rae, V. Sridhar, N. Wendland, B. W. Gregory, C. M. Johnson, *Int. Biodeterior. Biodegradation*, **127**, 146–159 (2018).
19. R. Bourbonnais, M. G. Paice, *Appl. Microbiol. Biotech.*, **36**, 823–827 (1992).
20. D. Daâssi, A. Prieto, H. Zouari-Mechichi, M. J. Martínez, M. Nasri, T. Mechichi, *Int. Biodeterior. Biodegradation*, **110**, 181–188 (2016).
21. M. Maryskova, I. Ardao, C. A. Garcia-Gonzalez, L. Martinova, J. Rotkova, A. Sevcu, *Enzyme Microbiol. Technol.*, **89**, 31–38 (2016).
22. L. Hongyan, Z. Zexiong, X. Shiwei, X. He, Z. Yinian, L. Haiyun, Y. Zhongsheng, *Chemosphere*, **224**, 743–750 (2019).
23. K. Piontek, M. Antorini, T. Choinowski, *J. Biol. Chem.*, **277**, 37663–37669 (2002).
24. X. Hou, J. Du, J. Zhang, L. Du, H. Fang, M. Li, *J. Chem. Inf. Model.*, **53**, 188–200 (2013).
25. A. P. Norgan, P. K. Coffman, J. P. A. Kocher, D. J. Katzmann, C. P. Sosa, *J. Cheminformatics*, **3**, 12 (2011).
26. M. A. Murcko, *J. Med. Chem.*, **38**, No. 26, 4953–4967 (1995).
27. Y. M. Cao, L. Xu, L. Y. Jia, *N. Biotechnol.*, **29**, 90–98 (2011).
28. R. A. Laskowski, M. B. Swindells, *J. Chem. Inf. Model.*, **51**, 2778–2786 (2011).

29. Y. Wei, Z. Yi, J. Xu, W. Yang, L. Yang, H. Liu, *J. Biomol. Struct. Dyn.*, **37**, 1402–1413 (2019).
30. J. Xu, Y. Wei, W. Yang, L. Yang, Z. Yi, *Analyst*, **143**, 4662–4673 (2018).
31. D. Wu, D. Liu, Y. Zhang, Z. Zhang, H. Li, *Eur. J. Med. Chem.*, **146**, 245–250 (2018).
32. A. E. Illera, S. Beltran, M. T. Sanz, *Sci. Rep.*, **9**, 13749 (2019).
33. Y. M. Song, J. Wu, X. R. Zheng, Q. Wu, *Chin. J. Inorg. Chem*., **22**, 1615–1622 (2006).
34. Principles of Fluorescence Spectroscopy, Ed. R. L. Joseph, Springer Science & Business Media, 529–569 (2013).
35. I. P. Caruso, W. Vilegas, M. A. Fossey, M. L. Cornelio, *Spectrochim. Acta A Mol. Biomol. Spectrosc.*, **97**, 449–455 (2012).
36. Z. A. Parray, F. Ahmad, M. I. Hassan, I. Hasan, A. Islam, *ACS Omega*, **5**, 13840–13850 (2020).
37. B. Nian, C. Cao, Y. Liu, *J. Chem. Technol. Biotech.*, **95**, 86–93 (2019).
38. S. K. Pawar, S. Jaldappagari, *J. Pharm. Anal.*, **9**, 274–283 (2019).
39. S. K. Pawar, R. Punith, R. S. Naik, J. Seetharamappa, *J. Biomol. Struct. Dyn.*, **35**, 3205–3220 (2017).
40. T. A. Wani, A. H. Bakheit, M. A. Abounassif, S. Zargar, *Front Chem.*, **6**, 47 (2018).
41. S. Li, J. H. Zhang, X. Y. Li, J. Q. Fu, *J. Beijing Institute Clothing Technol.*, **31**, 68–72 (2011).
42. G. Konstantin, I. Aymelt, S. G. Roger, G. Klaus, K. Carsten, *Biophys. Comp. Biol.*, **110**, 13380–13385 (2013).
43. Y. G. Shi, Q. Q. Guo, X. W. Yang, X. F. Liu, S. J. Wang, *J. Chin. Institute Food Sci. Tech.*, **18**, 225–231 (2018).
44. H. Tang, D. Zhao, *Bioorg. Chem.*, **88**, 102981 (2019).
45. Y. J. Kim, J. A. Nicell, *Bioresour. Technol.*, **97**, 1431–1442 (2006).
46. I. Escalona, J. de Grooth, J. Font, K. Nijmeijer, *J. Membrane Sci.*, **468**, 192–201 (2014).
47. J. Margot, J. Maillard, L. Rossi, D. A. Barry, C. Holliger, *New Biotech.*, **30**, 803–813 (2013).